Divertor heat flux characterisation during detachment experiments in TCV

R. Maurizio[1], B.P. Duval[1], O. Février[1], J. Harrison[2], B. Labit[1], B. Lipschultz[3], H. Reimerdes[1], C. Theiler[1], K. Verhaegh[1,3], W. Vijvers[4] , the TCV Team and the EUROfusion MST1 Team [1]

[1] *École Polytechnique Fédérale de Lausanne, Swiss Plasma Center, 1015 Lausanne, Switzerland*

[2] *CCFE, Culham Science Centre, OX14 3DB Abingdon, UK*

[3] *York Plasma Institute, University of York, York, YO10 5DD, UK*

[4] *Dutch Institute for Fundamental Energy Research (DIFFER), 5612 AJ Eindhoven, the Netherlands*

Introduction This work explores the evolution of target power load profiles during divertor detachment experiments in the TCV tokamak for L-mode Ohmic Lower Single-Null plasmas with the ion ∇B drift away from the X-point. The target heat flux is estimated by means of the Infrared (IR) Thermography system [2]. The detachment of the outer strike point (OSP) is achieved either by increasing the rate of N_2 injection in the private-flux region, at fixed line-averaged plasma electron density $\langle n_e \rangle$, or by increasing the density without impurity seeding. A decrease of the ion flux at the divertor plate, as measured by wall-embedded Langmuir probes (LPs), is conventionally taken at TCV as the indication of the onset of divertor detachment [3]. The inner strike point (ISP) remains attached during the density ramps but detaches when seeding N_2.

Nitrogen impurity seeding The plasma has a density of $\langle n_e \rangle = 8.8 \cdot 10^{19} m^{-3}$ ($\approx 41\%$ of the Greenwald density n_{GW}), a current of $I_P = 340\ kA$ and receives an Ohmic power of $P_\Omega = 540\ kW$. The target flux expansion is ≈ 3.5 and ≈ 4 at the inner and outer plates respectively, and the X-point poloidal distance from the vessel floor is $L_{div} = 41\ cm$. Nitrogen gas is injected by a valve located in the private flux region at $0.8\ s$, and the gas flux is ramped up to plasma disruption, figure 1a. The reconstructed exhausted power, i.e. the sum of the power at the divertor plates (measured with IR thermography) and radiated in the vessel volume (measured with bolometers), accounts for $\approx 80\%$ of P_Ω throughout the entire discharge. A relatively small impurity injection flux, $\Gamma_{N_2} \approx 10^{20} s^{-1}$, is sufficient to increase the radiative losses, figure 1b, and decrease the power deposited at the inner and outer divertor plates, figure 1c. Bolometric inversion indicates that the Nitrogen impurities radiate predominantly near the X-point and the inner target (not shown). This radiating region grows with the N_2 flux by intercepting an increasing fraction of the power flowing towards the targets. The rise of radiation coincides with a decrease of the ion flux to the outer and inner targets, figure 1d, the onset of divertor detachment. The fact that the ion

flux at the plate varies together with the power, for both divertors, may indicate that the intense radiative blob located at the X-point forces a decrease of the ionization source in the divertor volume and of the ion flux at the plate by limiting the power flowing into the ionization region.

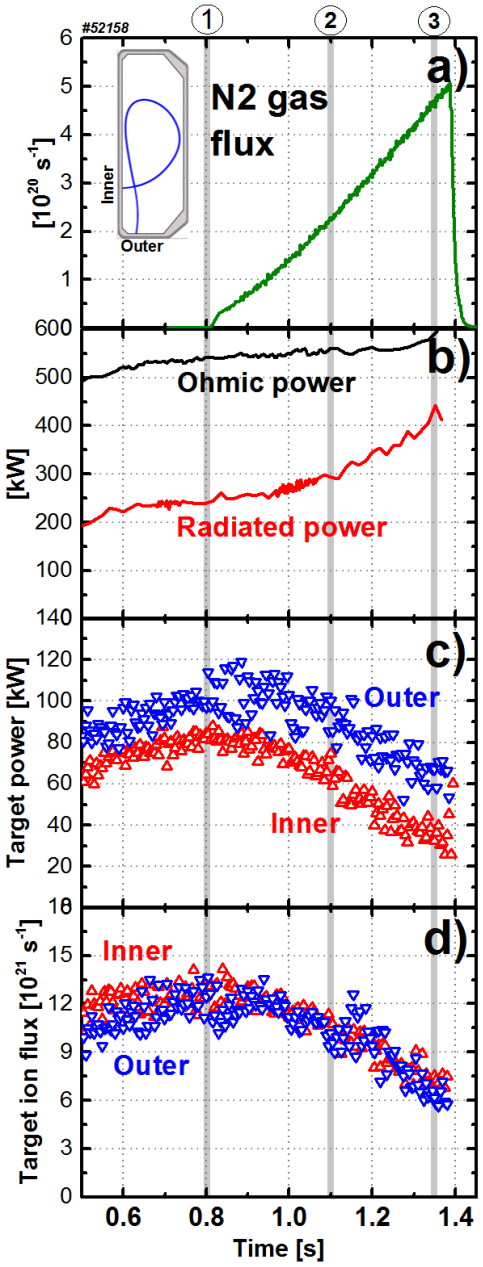

Figure 1: N_2 seeding experiment

Preliminary spectroscopic analysis confirms a decrease of the ionization source in the outer divertor with N_2 seeding, while signatures of recombination become visible only after the onset of detachment at ≈ 1 s and the recombination rate is at most a few percent of the ionization rate [4]. Seeding N_2 leads to a broadening of target heat flux profiles with the integral decay length $\lambda_{int,u}$ for both targets increasing by up to $\approx 50\%$ (not shown). In addition, the standard parameterisation of the heat load profiles [5] shows that only the SOL transport in the divertor is being affected, with a steady rise of the divertor spreading factor S_u for constant power fall-off length $\lambda_{q,u}$. According to a diffusive model for S_u in attached conditions [6, 2], the broadening S_u may reflect the decrease of the divertor electron temperature.

Plasma density ramp The plasma has a current of $I_P = 340\ kA$ while its density is ramped from 5 to $16 \cdot 10^{19} m^{-3}$ (25% to 74% of n_{GW}). The target flux expansion is ≈ 4 and ≈ 6 at the inner and outer target respectively, with $L_{div} = 39\ cm$. The reconstructed power accounts again for 80% of P_Ω throughout the density ramp. A higher density leads to an increase of the Ohmic power and also of the total radiated power P_{rad}, figure 2a. However, the rise in P_{rad} is stronger, and the radiated fraction P_{rad}/P_Ω steadily increases with density from 38% (OSP attached) to 65% just before the disruption (OSP detached). This is consistent with the drop of the power reaching the divertor plates, figure 2b, from 40% to 14% of P_Ω. The onset of OSP detachment takes place for a density of $\approx 1.1 \cdot 10^{20} m^{-3}$. The evolution of target power is significantly different between inner and outer divertor, for which an interpretation based on the radiation pattern is here proposed. The radiation pattern at the start of the density ramp (both divertors attached) features three blobs in

the divertor region (inner target, outer target and X-point) plus one at the outer mid-plane (not shown). With higher density, all the radiation blobs grow except the one at the outer target.

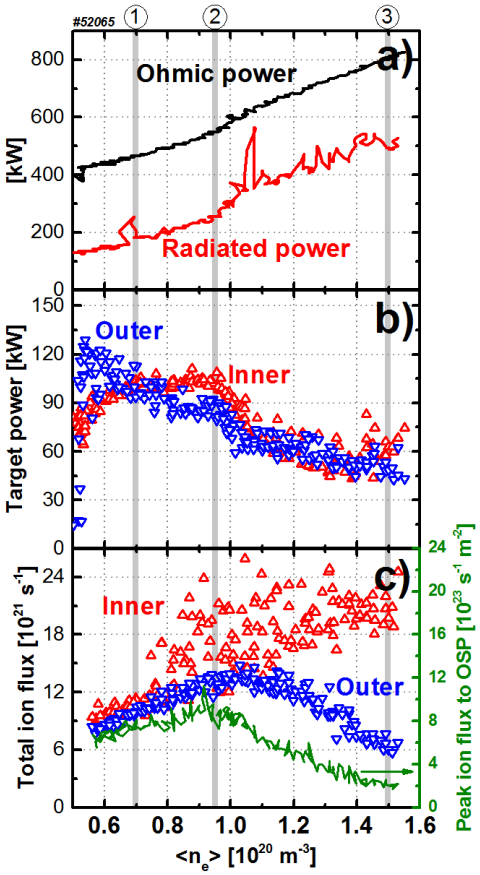

Figure 2: Density ramp experiment

Considering the outer SOL, this would suggest that the radiation blobs at the outer mid-plane and at the X-point efficiently dissipate an increasing fraction of the power flowing towards the ionization region in the outer leg. This would reduce the outer divertor ion source and could be the dominant mechanism for the roll-over of the target ion flux. Spectroscopic measurements in the outer divertor already excluded volumetric recombination processes from being the cause of the ion flux roll-over [7]. For the inner SOL, the target power starts dropping only at $\approx 0.95 \cdot 10^{20} m^{-3}$, which coincides with the roll-over of the peak ion flux at the outer strike point and with a pronounced increase of radiative losses in front of the ISP. Also, the peak of the heat flux profile at the inner divertor quickly drops to zero, creating a hollow profile (figure 3, the heat flux is mapped upstream at the OMP). A strong nonlinear behavior of the radiation in front of the target is a possible interpretation. Indeed, the ISP heat flux peak drops when the average temperature in the divertor leg is $\approx 8\ eV$, as indicated by the roll-over of the C-III line emission from the inner divertor leg from filtered tangential imaging (Multi-Cam), which roughly corresponds to the maximum of the Carbon cooling curve [8, 3].

The integral decay length at both targets increases by a factor 4 for the density range explored, Figure 4a, thus suggesting a stronger cross-field transport in the SOL with higher $\langle n_e \rangle$. Standard heat flux parameterisation starts failing after the onset of detachment because of the hollow profile at the ISP and the very low power reaching the OSP, shaded area in Figure 4. For the inner SOL and before detachment, the enhancement of cross-field transport is limited to the divertor region, as S_u increases while $\lambda_{q,u}$ is constant, Figure 4b and 4c. For the outer SOL, the enhancement of perpendicular transport involves both main and divertor SOL since both $\lambda_{q,u}$ and S_u increase

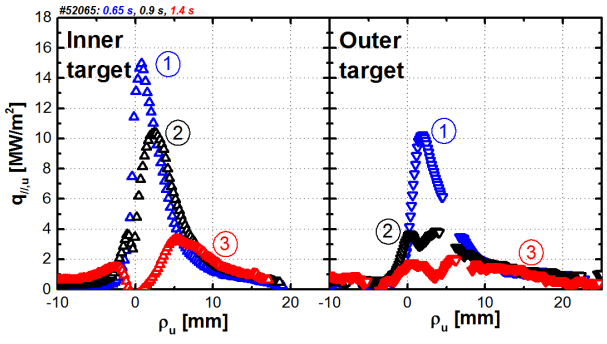

Figure 3: Target heat flux profiles

with the density. Also, the broadening of the outer SOL $\lambda_{q,u}$ is consistent with the broadening of the upstream density profile [9] and it may explain the growth of the radiating blob at the outer mid plane in terms of more C-sputtering due to an effectively smaller outer gap.

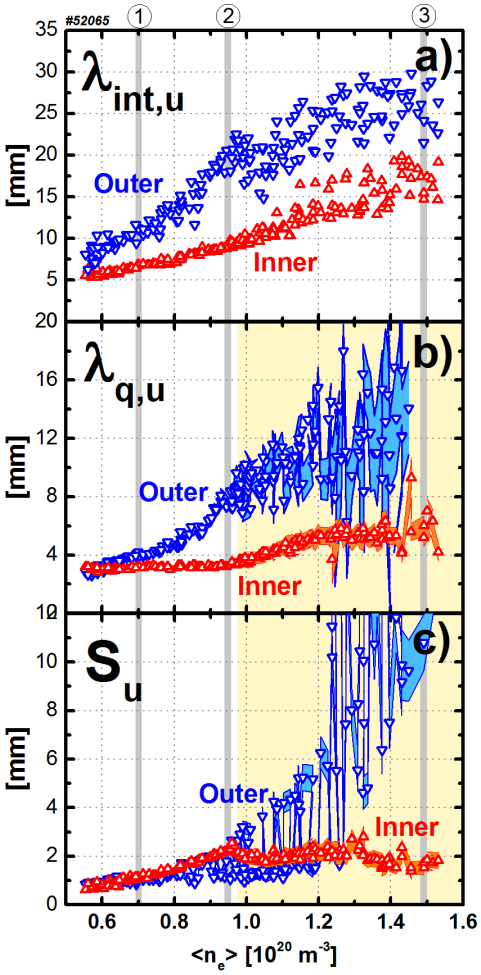

Figure 4: Target heat flux profile parameterisation

Conclusion The present study identifies two experimental features of divertor detachment in TCV achieved either by ramping the plasma density or the N_2 rate. The first is a reduction of the heat loads at the divertor plates relative to attached conditions, regardless of the approach adopted, which is in line with previous LP analysis [3] and with similar studies in other tokamaks [10]. The second feature consists in alterations of the target heat flux profile shape, which indicate an enhancement of cross-field transport in the SOL both before and after the onset of divertor detachment. The standard parameterisation of these profiles, which fails after the onset of detachment when a more complicated shape develops, reveals that the transport in the main and divertor SOL can be both enhanced, depending on the detachment scenario. The evolution of the radiation pattern and of power exhausted at the targets, together with spectroscopy analysis [4], suggest that the observed decrease of ion flux at the divertor plate might be predominantly caused in these experiments by a limitation of the power entering the ionization region in the divertor, for both detachment scenarios.

This work has been carried out within the framework of the EUROfusion Consortium and has received funding from the Euratom research and training programme 2014-2018 under grant agreement No 633053. The views and opinions expressed herein do not necessarily reflect those of the European Commission.

References

[1] Meyer H *et al*, Overview of progress in European Medium Sized Tokamaks towards an integrated plasma-edge/wall solution, accepted in NF
[2] Maurizio R *et al*, submitted to NF
[3] Theiler C *et al*, NF **57** (2017) 072008
[4] Verhaegh K *et al*, P4.123, this conference
[5] Eich T *et al*, PRL (2011)**107** 215001
[6] Sieglin B *et al*, PPCF (2016) **58** 055015
[7] Verhaegh K *et al*, NME (2017)
[8] Kallenbach A *et al*, PPCF **55** (2013) 124041
[9] Harrison J *et al*, NME 2016
[10] Kallenbach A *et al*, NF **55** (2015) 053026